

WRC-1992 Constitution Diagram for Stainless Steel Weld Metals: A Modification of the WRC-1988 Diagram

Refined constitution diagram offers more accurate FN prediction for Cu-containing stainless steels and dissimilar metal joints

BY D. J. KOTECKI AND T. A. SIEWERT

ABSTRACT. To increase the scope and accuracy of Ferrite Number (FN) prediction in stainless steel weld metal and related dissimilar metal joints, a modification of the Welding Research Council 1988 diagram (WRC-1988 diagram) is proposed. The proposed WRC-1992 diagram includes a coefficient for Cu in the Ni equivalent, thereby removing a tendency for the WRC-1988 diagram to overestimate the FN of weld metals when the Cu content is high. Also, the axes of the WRC-1992 diagram can be extended (as in the Schaeffler diagram) to predict dilution effects in dissimilar metal joints.

Introduction

The prediction of the microstructures and properties (such as hot cracking and corrosion resistance) for the austenitic stainless steels has been the topic of many studies. A 1985 review by Olson (Ref. 1) lists 169 references on microstructure and property prediction for austenitic weld metal. During the last two decades, two of the microstructure prediction diagrams have found the widest application.

The Schaeffler diagram (Fig. 1), published in 1949, has been extensively used for estimating the ferrite content of stainless steel weld metals (Ref. 2). The diagram contains phase fields and iso-ferrite lines that permit prediction of the weld structure from the composition. It is still widely used for predicting the ferrite content of dissimilar metal weld deposits. Briefly, this involves calculating a "chromium equivalent" (Cr_{eq}) and a "nickel equivalent" (Ni_{eq}) for each base

metal and for the proposed filler metal, plotting each equivalent on the Schaeffler diagram, and drawing tie lines between the plotted points, proportioned according to expected dilution, to obtain an estimate of the weld metal ferrite content. This has been a valuable tool for estimating the physical and mechanical properties of a weld.

Several problems have been identified when using the Schaeffler diagram for this purpose, however. The Schaeffler diagram does not consider the powerful effect of N in promoting austenite at the expense of ferrite, and is incorrect in its treatment of Mn. Manganese does not promote the high-temperature formation of austenite at the expense of ferrite, as predicted by the diagram, although Mn does stabilize austenite in its low-temperature transformation to martensite. Also, the Schaeffler diagram makes its predictions in terms of "percent ferrite." Later, this was found to be imprecise and the magnetically based "Ferrite Number" (FN) unit was developed for the specification and determination of ferrite content. The basis for the FN scale is described in standards ANSI/AWS A4.2 and ISO 8249.

The other widely used prediction diagram, the DeLong diagram (Ref. 3), was published in 1974 and incorporated some improvements. It has an FN scale

and includes a coefficient for N in the Ni_{eq} , though the range of compositions is more limited than for the Schaeffler diagram. In effect, the DeLong diagram traded improved prediction accuracy for a more limited composition range, but a range that included all the common austenitic stainless steel weld metals. However, it has been found to incorrectly handle Mn (as did the Schaeffler diagram) and to overestimate the FN of more highly alloyed compositions, such as Type 309 (Ref. 4). It also had limited application to dissimilar metal joints.

The recently developed WRC-1988 diagram (Ref. 4) overcomes many of the problems associated with the Schaeffler and DeLong diagrams. It was developed with data measured by the most recent definition of the FN scale, it removed the erroneous Mn coefficient from the Ni_{eq} , and eliminated the systematic overestimation of FN for highly alloyed weld metals. While it covers a much broader range of compositions than does the DeLong diagram, it has a narrower composition range than the Schaeffler diagram, because it extends only over the composition range of the commercial alloys (and experimental compositions that were minor modifications of commercial alloys) with which it was developed.

In the interval since the WRC-1988 diagram first appeared, it has been subject to evaluation and review. Independent data from over 200 weld metals have confirmed the improved prediction accuracy of the WRC-1988 diagram over that of its predecessors (Ref. 5). As a result, the WRC-1988 diagram is being considered to replace the DeLong diagram in the ASME Boiler and Pressure Vessel Code.

Effect of Cu on Ferrite Number

In recent years, duplex ferritic-austenitic stainless steels have been used more frequently. Some of these steels, and their weld metals, contain significant amounts of Cu (often about 2%). While these compositions might be plotted on

KEY WORDS

Ferrite Number
WRC-1992 Diagram
WRC-1988 Diagram
Stainless Steel
Cu Coefficient
Ni Equivalent
Dilution
SS Weld Metals
Dissimilar Joints
Ferrite Prediction

D. J. KOTECKI is Technical Director for Stainless and High Alloy Product Development, The Lincoln Electric Co., Cleveland, Ohio. T. A. SIEWERT is Group Leader, Materials Reliability Div., National Institute of Standards and Technology, Boulder, Colo.

Contribution of NIST not subject to copyright.

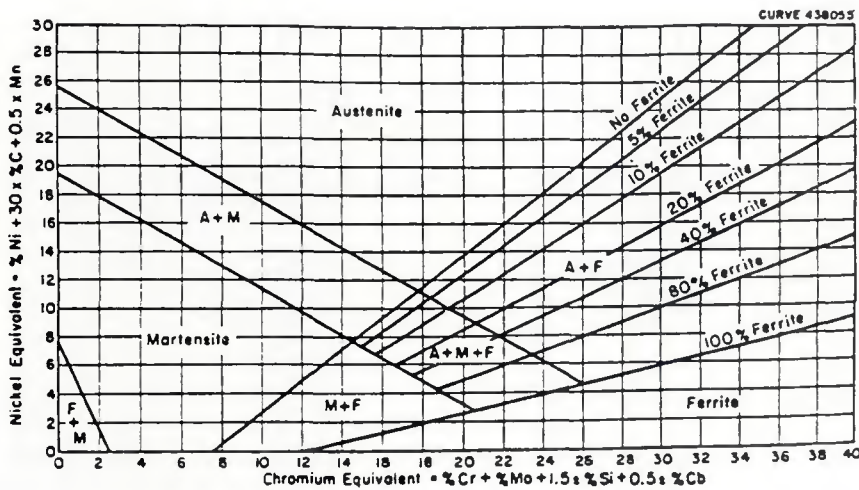


Fig. 1 — Schaeffler diagram (Ref. 2).

the existing WRC-1988 diagram with reasonable accuracy, Lake (Ref. 6) has shown that a coefficient for Cu will improve the accuracy for weld metals in which Cu is an important alloying element. One purpose of this paper is to examine the effect of Cu, using data developed by both Lake and Kotecki. These data allow comparison of the calculated FN with measured FN for ferritic-austenitic weld metals over a range of Cu.

A coefficient for Cu in the Ni_{eq} of the Schaeffler or DeLong diagrams has been proposed by various researchers. Hull has proposed a coefficient of 0.44 (Ref. 7), Castro and deCadenet proposed a coefficient of 0.6 (Ref. 8), Potak and Sagalevich proposed a coefficient of 0.5 (Ref. 9), and Ferree proposed a coefficient of 0.3 (Ref. 10). These reports suggest the effect of Cu is significant and

should be considered when predicting FN.

During development of the WRC-1988 diagram, a Cu coefficient was sought, but no trend was evident. The majority of the Cu data that was submitted were for weld metals of low-FN and low-Cu content (less than 0.3% Cu). About 20 of the duplex ferritic-austenitic compositions included Cu above 1%, but there were little data for duplex compositions with low Cu for comparison. Thus, it is likely that any effect of Cu was statistically confounded with the FN effect. This conclusion is supported by the Cu term that appeared in some of the analyses (on various subsets of the database) during the development of the WRC-1988 diagram, but the calculated coefficients for Cu differed widely, and each had a large uncertainty (Ref. 11).

Lake (Ref. 6) developed data

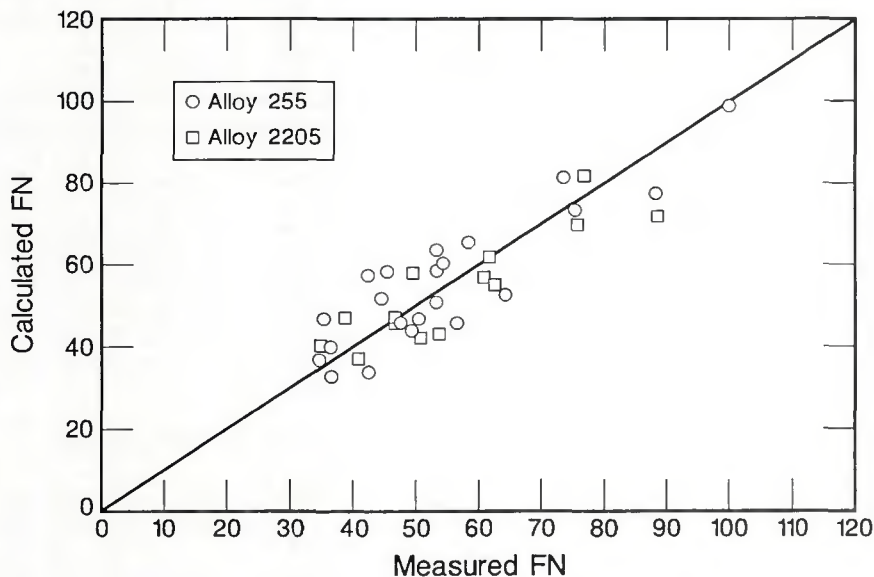


Fig. 2 — Data for the predicted vs. measured FN values using a coefficient of 0.25 for Cu.

specifically for evaluation of the effect of Cu in the WRC-1988 diagram. His data have a uniform distribution over the range of 0 to 4% Cu, which permits accurate determination of the effect of Cu. Further, Lake's data are well distributed around the WRC-1988 diagram, which permits examination of the effect of Cu in different solidification modes and FN ranges. He found the effect of Cu on the Ni_{eq} to be linear and fairly uniform regardless of the location within the WRC-1988 diagram. As a result, Lake proposed adding a Cu term to the Ni_{eq} of the WRC-1988 diagram. For various austenitic weld metals containing some ferrite, this contribution to the Ni_{eq} amounted to a coefficient of 0.25 to 0.30 to be multiplied by the % Cu in the weld metal. The contribution is then added to the original Ni_{eq} as calculated according to the WRC-1988 diagram (Ref. 4).

Using Lake's data as a basis, Kotecki (Ref. 12) proposed a coefficient for Cu of 0.25 in the Ni_{eq} equivalent and prepared a table of calculated vs. measured FN for a series of compositions based on 22Cr-5Ni-3Mo-N (Alloy 2205) and 25Cr-5Ni-3Mo-2Cu-N (Alloy 255) duplex ferritic-austenitic weld metals. For convenience, this is reproduced as Table 1. Two regressions of measured FN vs. calculated FN were performed on these data, as indicated at the bottom of Table 1. In the first, a nonzero intercept (constant) and a slope were permitted. When the standard error of an FN estimate was observed to be greater than the calculated intercept (implying that the term is not statistically significant), a second regression was performed in which the line was forced through the origin (intercept of zero). In this second regression, the fit (R-squared) is nearly the same as in the first regression, and the slope is very close to 1, with a very small standard error. The data are then plotted in Fig. 2 with different symbols that identify which points are for Alloy 255 (weld metals containing about 2% Cu), and which points are for Alloy 2205 (weld metals containing very little Cu). As can be seen in Fig. 2, all of the data fall along a 1:1 line, and there appears to be no clustering of points with or without Cu on either side of the 1:1 line.

If the contribution of Cu to the Ni_{eq} were omitted, the calculated Ni equivalent for every Alloy 255 weld metal would be about 0.5 less than is given in Table 1, and the resulting calculated Ferrite Numbers for the Alloy 255 weld metals would therefore be on the order of 7 FN greater than the values given in Table 1. Then virtually all of the Alloy 255 data points would be above the 1:1 line of Fig. 2, indicating a bias. The good fit of the line in Fig. 2 indicates that the coefficient developed by Lake for Cu in

the Ni_{eq} of the WRC-1988 diagram is, at least to a first approximation, quite suitable and useful for estimating ferrite content in these weld metals. Therefore, we propose a new WRC-1992 diagram which is exactly the same as the WRC-1988 diagram, except that the new Ni_{eq} includes a Cu term. This WRC-1992 diagram is presented as Fig. 3.

Extension of the WRC-1992 Diagram

Whereas the Schaeffler diagram offers predictions for Cr_{eq} from 0 to 40 and Ni_{eq} from 0 to 32, the WRC-1992 diagram is more limited, considering Cr_{eq} from 17 to 31 and Ni_{eq} from 9 to 18. The second purpose of this paper is to demonstrate how the axes of the WRC-1992 diagram can be extended to predict the FN for dissimilar metal joints, over at least as broad a range as covered by the Schaeffler diagram. The examples below illustrate the calculations.

Although Ferrite Numbers do not exist for weld deposits of low Cr_{eq} and Ni_{eq} , the positions of such alloys can still be located by extrapolated Cr_{eq} and Ni_{eq} units on the WRC-1992 diagram. Dilution calculations are based on linear combinations of the compositions, and the extended axes of the diagram allow visualization of the concept. This procedure is illustrated in Figs. 4 and 5, and described in the following paragraphs. The graphical procedure is exactly the same as that used with the Schaeffler diagram. While the extended axes allow a wide range of initial compositions to be located, the FN prediction is only accurate for weld compositions (the compositions that result from mixing and dilution of the initial compositions) that fall within the bounds of the iso-FN lines (0 to 100 FN) drawn on the diagram. The boundaries of the FN lines were determined by the extent of the database, and extension of the straight FN isopleths into the adjacent Cr_{eq} and Ni_{eq} regions could result in erroneous predictions.

For some Cr_{eq} and Ni_{eq} values beyond the lower limits of the FN lines in the WRC-1992 diagram, martensite may be found in the weld metals. In the Schaeffler diagram, such weld metals were indicated below and to the left of a diagonal line — Fig. 1. In contrast to the Schaeffler diagram, Mn does not appear in the Ni_{eq} of the WRC-1992 diagram because it is not found to affect significantly the high-temperature transformation of ferrite to austenite. However, the more recent findings of Self, Matlock and Olson (Ref. 13) show that Mn stabilizes austenite with respect to low-temperature transformation to

Table 1—Measured FN vs. FN Calculated by WRC-88 Diagram, Data from Ref. 12 $Ni_{eq} + 0.25$ (%Cu)

Weld Number	Type	Cr_{eq}	Ni_{eq}	Calculated FN	Measured FN	Measured Minus Calculated FN
9292-622	255	28.61	15.81	36	34	-2
9276-999	2205	25.25	12.57	39	34	-5
9276-057	255	28.14	14.57	46	35	-11
9276-014	255	28.70	16.33	32	36	4
9292-678	255	29.69	16.46	39	36	-3
9276-998	2205	25.79	12.57	46	38	-8
9276-854	2205	23.13	10.81	36	40	4
9292-650	255	28.32	15.93	33	42	9
9292-136	255	26.70	12.54	57	42	-15
9276-056	255	28.43	14.30	51	44	-7
9292-112R	255	27.69	13.20	58	45	-13
9276-996	2205	25.33	12.24	45	46	1
9292-109	2205	24.75	11.70	46	46	0
9276-012	255	28.03	14.57	45	47	2
9276-013	255	28.24	14.94	43	49	6
9276-864	2205	25.61	11.66	57	49	-8
9276-984	2205	25.18	12.36	41	50	9
9292-174	255	27.08	13.70	46	50	4
9276-997	2205	25.56	12.62	42	53	11
9292-358	255	29.66	15.32	50	53	3
9292-137	255	27.08	12.74	58	53	-5
9292-112	255	27.69	12.88	63	53	-10
9292-203	255	28.09	13.38	60	54	-6
9276-004	255	27.69	14.29	45	56	11
9292-231	255	28.53	13.36	65	58	-7
9276-904	2205	25.95	12.03	56	60	4
9276-863	2205	25.63	11.44	61	61	0
9276-853	2205	23.72	10.36	54	62	8
9292-161	255	27.19	13.24	52	64	12
9276-053	255	29.55	12.78	81	73	-8
9276-817	2205	24.02	9.81	69	75	6
9276-055	255	28.71	12.78	73	75	2
9276-844	2205	24.08	9.39	81	76	-5
9292-204	2205	25.71	10.92	71	88	17
9276-054	255	29.49	12.99	77	88	11
9292-202	255	28.19	10.66	99	100	1

Regression: Measured vs. Calculated FN

Constant	3.663357
Std Err of Y Est	7.990919
R Squared	0.769152
No. of Observations	36
Degrees of Freedom	34
X Coefficient(s)	0.938617
Std Err of Coef.	0.088187

Regression: Measured vs. Calculated FN

Constant	0
Std Err of Y Est	7.938712
R Squared	0.765457
No. of Observations	36
Degrees of Freedom	35
X Coefficient(s)	1.001287
Std Err of Coef.	0.023495

martensite. Because of the differing effects of Mn in the two temperature ranges, it is not possible to include a single line bounding martensite-containing weld metals on the WRC-1992 diagram.

Example 1: Overlay of AISI 1050 steel with AWS A5.4 Class E312-16 electrode.

Table 2 lists typical plate composition and all-weld-metal composition produced with this electrode. The Cr_{eq}

and Ni_{eq} for the AISI 1050 steel (0.0 and 17.50, respectively) do not permit an FN calculation for this material. The Cr_{eq} and Ni_{eq} for the E312-16 electrode all-weld-metal composition (29.0 and 11.9, respectively) result in a predicted 88.2 FN for this material. If the Cr_{eq} and Ni_{eq} for each composition is plotted in Fig. 4 and a line is drawn between the point corresponding to the AISI 1050 composition (Point A in Fig. 4) and the point corresponding to the E312-16 composi-

Table 2—Cladding of AISI 1050 with E312-16

Material	AISI 1050	E312-16 All-Weld-Metal	30% Dilution Cladding
C %	0.50	0.060	0.192
Mn %	0.30	1.20	0.93
Si %	0.02	0.60	0.43
Cr %	—	29.00	20.30
Ni %	—	8.60	6.02
N %	0.004	0.06	0.043
Cr _{eq}	0.00	29.00	20.30
Ni _{eq}	17.58	11.90	13.60
WRC-1988 FN	—	88.2	4.6

Table 3—Joining 304 to A36 with E309L-16

Material	AISI 304	ASTM A36	E309L-16 All-Weld-Metal	70% E309L-16, 15% AISI 304, 15% A36
C %	0.05	0.20	0.03	0.059
Mn %	1.60	0.80	1.40	1.34
Si %	0.40	0.20	0.60	0.51
Cr %	18.75	—	24.40	19.89
Ni %	9.90	—	12.70	10.38
Mo %	0.08	—	0.20	0.15
N %	0.04	0.004	0.06	0.049
Cr _{eq}	18.83	0.00	24.60	20.04
Ni _{eq}	12.45	7.08	14.95	13.39
WRC-1988 FN	3.2	—	17.4	4.3

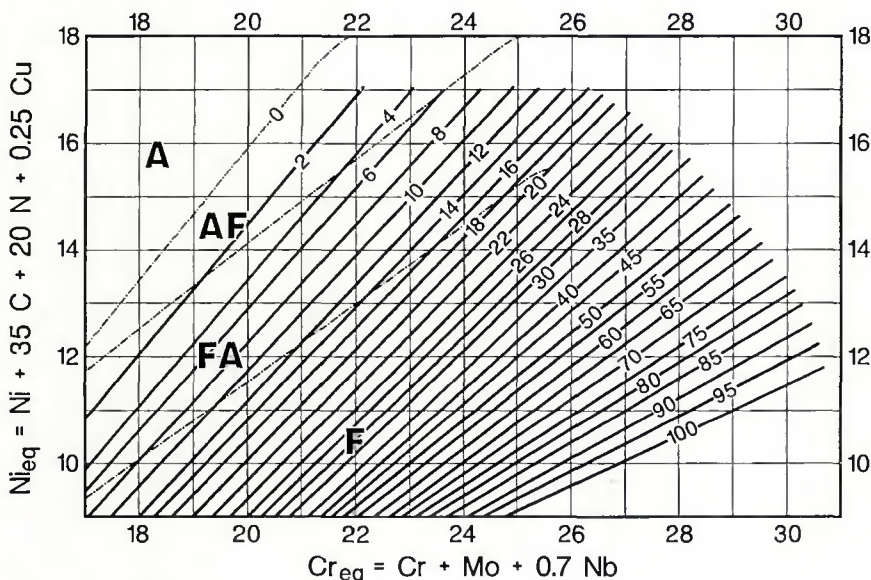


Fig. 3 — WRC-1992 diagram.

tion (Point B in Fig. 4), then all possible mixtures of these two materials must lie along this line.

The lever rule is then used to estimate the position of the weld metal. In shielded metal arc welding, typical dilution is 30%. A weld pass of E312-16 with 30% dilution from AISI 1050 steel would lie at a Point C, located 30% of the distance from Point B to Point A in Fig. 4. Mathematically, this can be calculated as

$$Cr_{eq}(C) = 0.7 Cr_{eq}(B) + 0.3 Cr_{eq}(A) = 0.7(29.00) + 0.3(0.00) = 20.30,$$

$$Ni_{eq}(C) = 0.7 Ni_{eq}(B) + 0.3 Ni_{eq}(A) = 0.7(11.90) + 0.3(17.58) = 13.60.$$

The Cr_{eq} and Ni_{eq} of Point C correspond to 4.6 FN, which indicates that the weld pass will have sufficient FN to avoid fissuring (Ref. 4). Any additional passes, overlapping part of this first pass, will also lie along the line between Point B and Point A, but they will be closer to Point B than is Point C, so all subsequent

passes will contain even more ferrite than the first pass, and the weld cladding should be crack-free.

Example 2: Joining AISI 304 Stainless Steel to ASTM A36 with E309L-16 Electrode.

Table 3 lists typical plate compositions and all-weld-metal composition from the electrode. The Cr_{eq} and Ni_{eq} for the A36 steel (0.00 and 7.08, respectively) do not permit an FN calculation for this material. The Cr_{eq} and Ni_{eq} for the AISI 304 steel (18.83 and 12.45, respectively) result in a calculated 3.2 FN for this material. The Cr_{eq} and Ni_{eq} for these two base metals are shown in Fig. 5 as Point D (A36) and Point E (304). Any mixture of these two base metals will lie along the line connecting Point D to Point E. If each base metal contributes equally to the weld metal, then the overall base metal contribution is given by the midpoint of the line between Point D and Point E, indicated in Fig. 5 as Point F. If one base metal contributed more than the other to the joint

(due to unequal plate thickness of a complex joint design, for example), then Point F would slide along this line proportionately toward the greater contributor. In any case, the average base metal contribution to the weld pool would lie along this line.

The all-weld-metal Cr_{eq} and Ni_{eq} (24.60 and 14.95, respectively) for the E309L-16 electrode is shown as Point G in Fig. 5, and a 17.4 FN would be predicted for that electrode. The root pass weld metal, consisting of the E309L-16 electrode and equal parts of the two base metals, must lie along the line from Point G to Point F in Fig. 5. Again assuming normal 30% base metal dilution with the shielded metal arc process, the root pass weld would lie 30% of the distance along the line from Point G to Point F. This is shown as Point H in Fig. 5. The calculations to reach Point H are shown below.

$$Cr_{eq}(F) = 0.5 Cr_{eq}(D) + 0.5 Cr_{eq}(E) = 0.5(0.00) + 0.5(18.83) = 9.47$$

$$Ni_{eq}(F) = 0.5 Ni_{eq}(D) + 0.5 Ni_{eq}(E) = 0.5(7.08) + 0.5(12.45) = 9.77$$

$$Cr_{eq}(H) = 0.7 Cr_{eq}(G) + 0.3 Cr_{eq}(F) = 0.7(24.60) + 0.3(9.47) = 20.04$$

$$Ni_{eq}(H) = 0.7 Ni_{eq}(G) + 0.3 Ni_{eq}(F) = 0.7(14.95) + 0.3(9.77) = 13.39$$

Point H corresponds to 4.3 FN, which would be expected to result in a crack-free root pass in this joint. Higher dilution, or excess dilution from the A36 side of the joint, could reduce the ferrite content and increase the likelihood of cracking.

It is not necessary actually to plot the calculated Cr_{eq} and Ni_{eq} for the base metals and electrode on the extended WRC-1992 diagram in order to obtain useful information. After calculation of the Cr_{eq} and Ni_{eq}, only the final weld metal need be plotted on the WRC-1992 diagram to obtain a weld metal FN prediction. However, plotting all the data

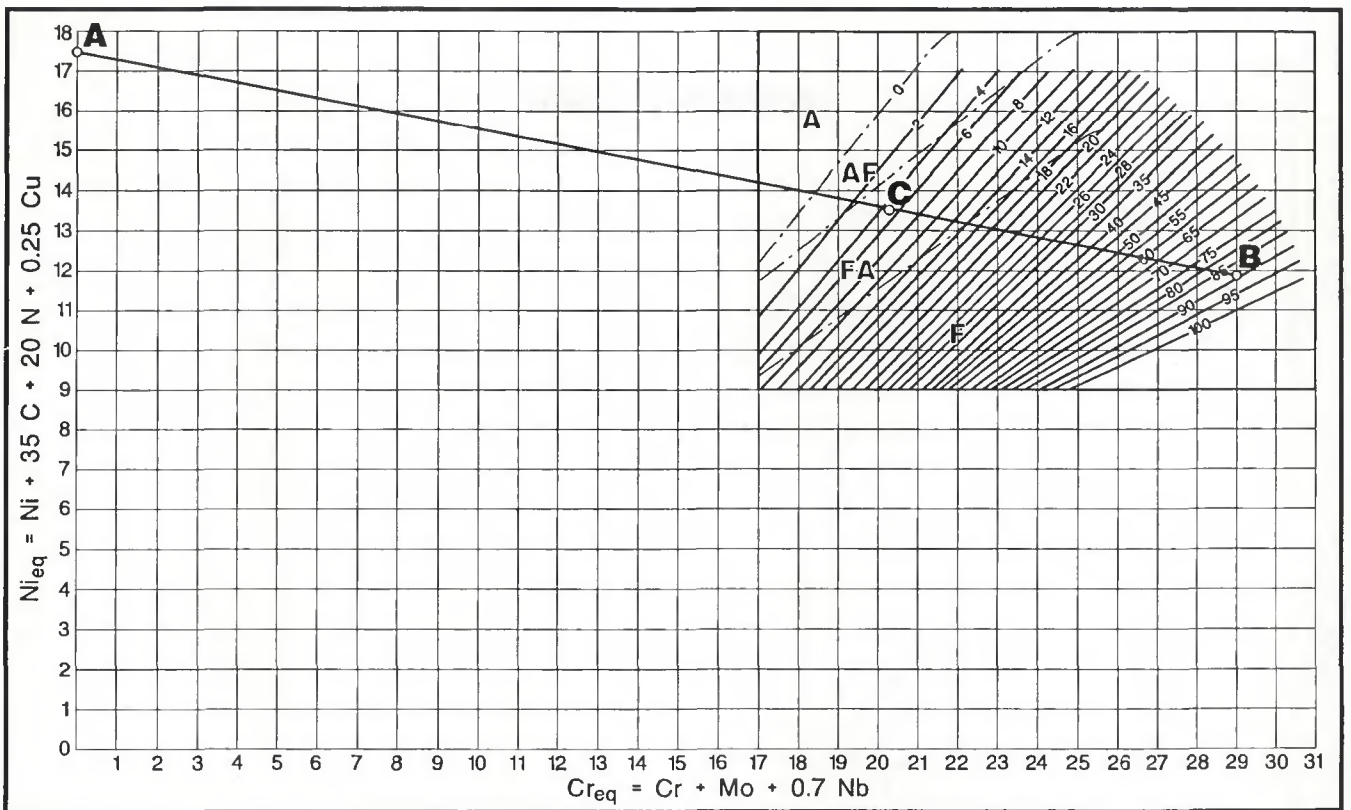


Fig. 4 — Illustration of dilution calculation in Example 1.

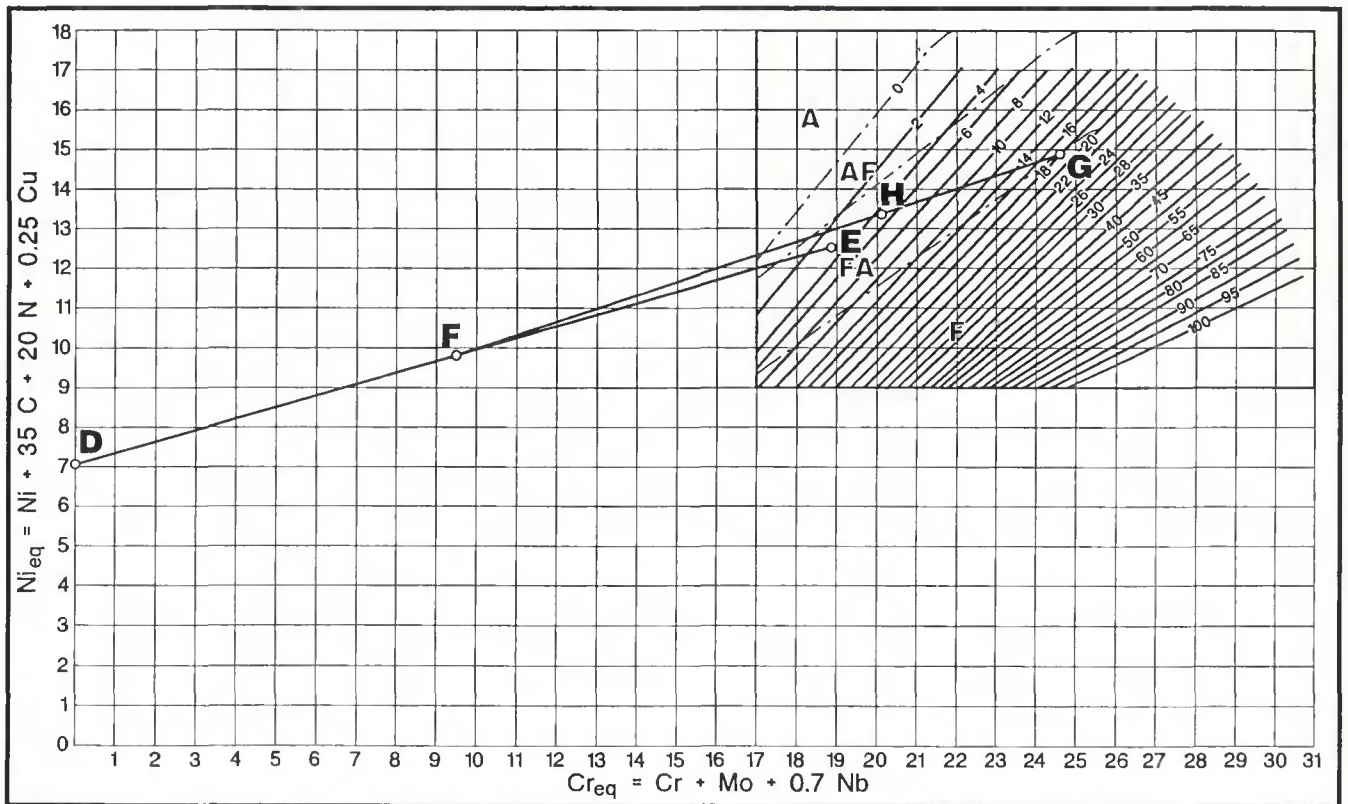


Fig. 5 — Illustration of dilution calculation in Example 2.

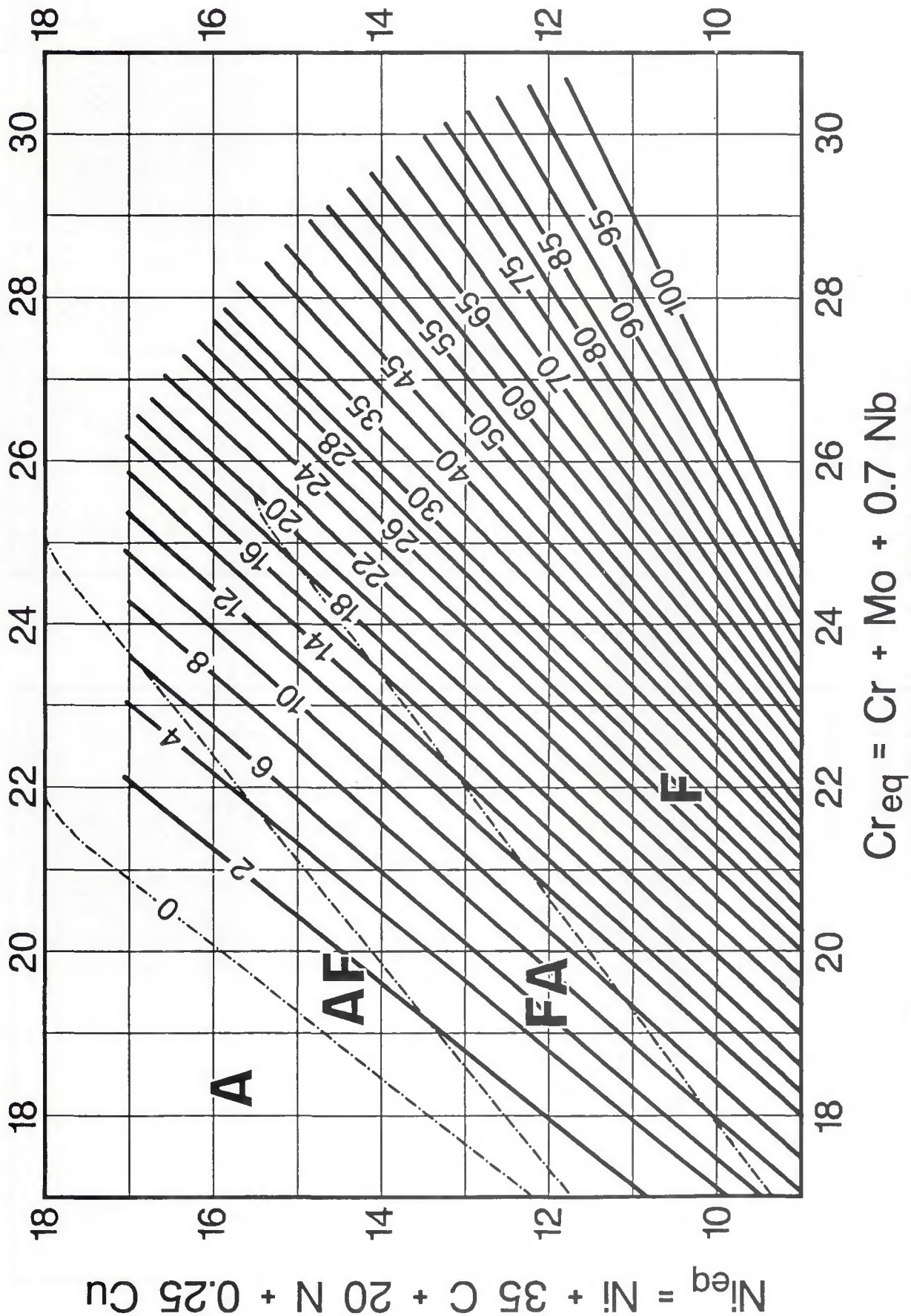


Fig. 6. — WRC-1992 diagram. The FN prediction is only accurate for weld compositions that fall within the bounds of the iso-FN lines (0 to 100 FN) that are drawn on the diagram. The limits of the diagram were determined by the extent of the database, and extension of the lines could result in erroneous predictions.

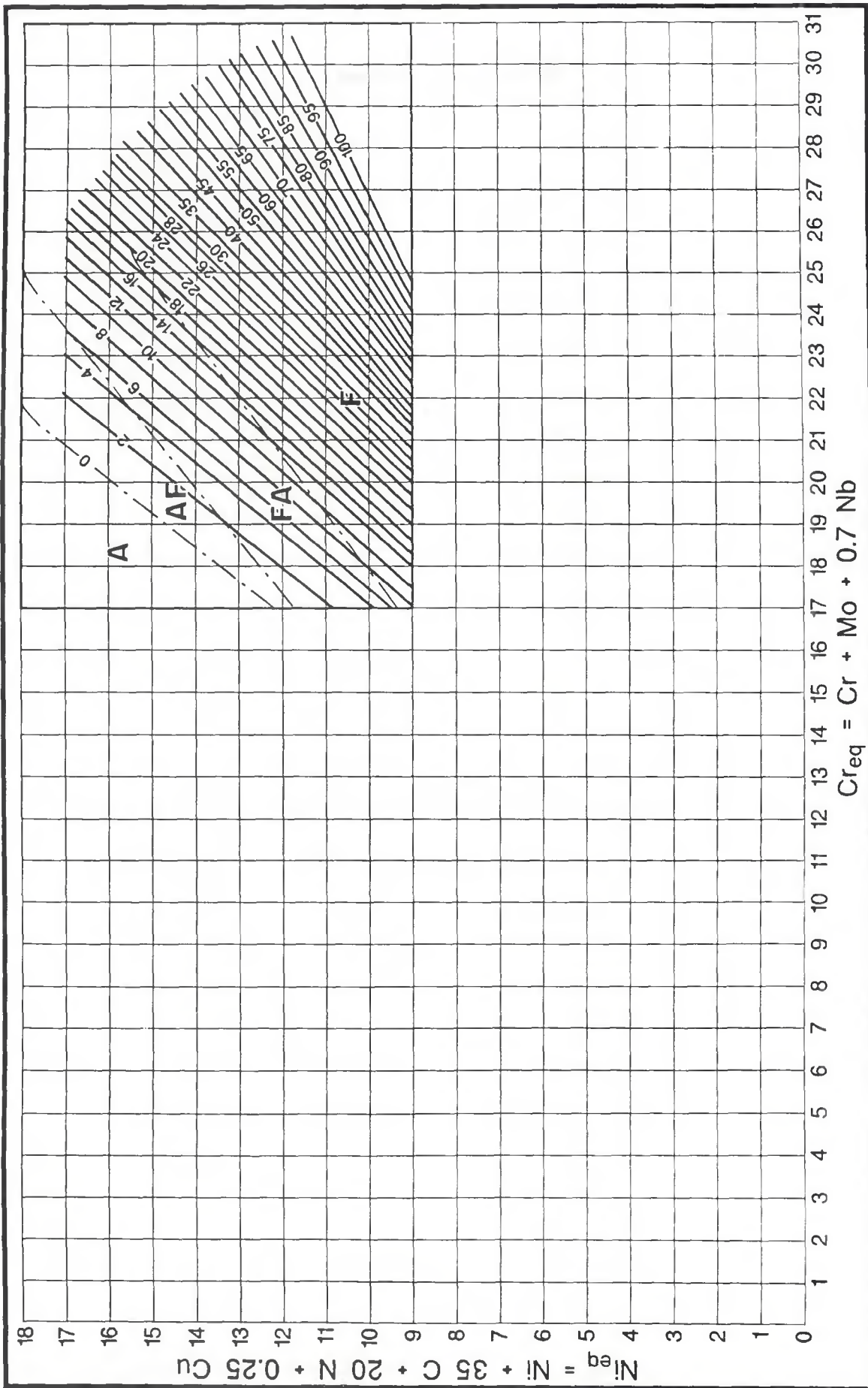


Fig. 7. — WRC-1992 diagram with an expanded scale for dilution calculations. While the extended axes allow a wide range of compositions to be located, the FN prediction is only accurate for weld compositions that fall within the bounds of the iso-FN lines (0 to 100 FN) that are drawn on the diagram. The limits of the WRC diagram were determined by the extent of the database, and extension of the lines could result in erroneous predictions.

on the diagram is useful in that it gives a clearer picture of the situation, so that one can appreciate the risks of higher than expected dilution.

It is also possible to extend the WRC-1992 diagram to higher Ni_{eq} , to examine dissimilar metal joints involving nickel-base alloys. It is reasonable to expect that other combinations could be found that would produce weld metal compositions falling within the limits of the diagram.

To facilitate the use of this new diagram, Figs. 6 and 7 are copies of the WRC-1992 diagram and an extended version for dissimilar metal weld predictions.

Conclusions

We propose a new diagram, the WRC-1992 diagram for the FN prediction of stainless steel welds. It improves the FN prediction accuracy for stainless steel weld metals that have significant Cu contents. For welds with low-Cu contents, its predictions are not significantly different from those of the WRC-1988

diagram.

We also offer the diagram on extended axes (similar to the range of the Schaeffler diagram) for improved prediction of FN for dissimilar weld and cladding applications.

References

1. Olson, D. L. 1985. Prediction of austenitic weld metal microstructure and properties. *Welding Journal* 64(10):281-s to 295-s.
2. Schaeffler, A. L. 1949. Constitution diagram for stainless steel weld metal. *Metal Progress* 56(11):680-680B.
3. DeLong, W. T. 1974. Ferrite in austenitic stainless steel weld metal. *Welding Journal* 53(7):273-s to 286-s.
4. Siewert, T. A., McCowan, C. N., and Olson, D. L. 1988. Ferrite number prediction to 100 FN in stainless steel weld metal. *Welding Journal* 67(12):289-s to 298-s.
5. Kotecki, D. J. 1988. Verification of the NBS-CSM ferrite diagram. International Institute of Welding Document II-C-834-88.
6. Lake, F. B. 1990. Effect of Cu on stainless steel weld metal ferrite content, Paper presented at AWS Annual Meeting.

7. Hull, F. C. 1973. Delta ferrite and martensite formation in stainless steels. *Welding Journal* 52(5):193-s to 203-s.

8. Castro, R. J., and deCadenet, J. J. 1974. *Welding Metallurgy of Stainless and Heat Resisting Steels*. Cambridge University Press, Cambridge, U.K.

9. Potak, M., and Sagalevich, E. A. 1972. Structural diagram for stainless steels as applied to cast metal and metal deposited during welding. *Avt. Svarka* (5):10-13.

10. Ferree, J. A. 1969. Free machining austenitic stainless steel. U.S. Patent 3,460,939.

11. McCowan, C. N., Siewert, T. A., and Olson, D. L. 1989. Stainless steel weld metal: Prediction of ferrite content. WRC Bulletin 342, Welding Research Council, New York, N.Y.

12. Kotecki, D. J. 1990. Ferrite measurement and control in duplex stainless steel welds. *Weldability of Materials — Proceedings of the Materials Weldability Symposium*, October, ASM International, Materials Park, Ohio.

13. Self, J. A., Matlock, D. K., and Olson, D. L. 1984. An evaluation of austenitic Fe-Mn-Ni weld metal for dissimilar metal welding. *Welding Journal* 63(9):282-s to 288-s.

WRC Bulletin 370 February 1992

Recommendations Proposed by the PVRC Committee on Review of ASME Nuclear Codes and Standards Approved by the PVRC Steering Committee

The ASME Board on Nuclear Codes and Standards (BNCS) determined in 1986 that an overall technical review of existing ASME nuclear codes and standards was needed. The decision to initiate this study was reinforced by many factors, but most importantly by the need to capture a pool of knowledge and "lessons learned" from the existing generation of technical experts with codes and standards background.

Project responsibility was placed with the Pressure Vessel Research Council and activity initiated in January 1988. The direction was vested in a Steering Committee which had overview of six subcommittees.

The recommendations provided by nuclear utilities and industry were combined with the independent considerations and recommendations of the PVRC Subcommittees and Steering Committees.

Publication of this document was sponsored by the Steering Committee on the Review of ASME Nuclear Codes and Standards of the Pressure Vessel Research Council. The price of WRC Bulletin 370 is \$30.00 per copy, plus \$5.00 for U.S. and \$10.00 for overseas, postage and handling. Orders should be sent with payment to the Welding Research Council, Room 1301, 345 E. 47th St., New York, NY 10017.